Dalton Transactions

An international journal of inorganic chemistry

Accepted Manuscript

This article can be cited before page numbers have been issued, to do this please use: T. Hashemzadeh, M. Haghighatbin, J. Agugiaro, C. F. Hogan, D. J. Wilson and P. Barnard, *Dalton Trans.*, 2020, DOI: 10.1039/D0DT02177F.

ROYAL SOCIETY OF CHEMISTRY

rsc.li/dalton

Luminescent Iridium(III)-Boronic Acid Complexes for Carbohydrate Sensing

View Article Online
DOI: 10.1039/D0DT02177F

Tahmineh Hashemzadeh, Mohammad A. Haghighatbin, Johnny Agugiaro, David D. J. Wilson, Conor F. Hogan and Peter J. Barnard*

Department of Chemistry and Physics, La Trobe Institute for Molecular Science, La Trobe University, Victoria, 3086, Australia, E-mail: p.barnard@latrobe.edu.au

Abstract

A family of four Ir(III) complexes of the form $[Ir(ppy)_2(L)]Cl$ (where ppy = 2-phenyl-pyridine and L = a pyridyl-1,2,4-triazole or pyridyl-1,3,4-oxadiazole ligand bearing a boronic acid group) have been prepared as potential luminescent sensors for carbohydrates. A modular eight step procedure was developed to synthesise the complexes, and this was initiated with the preparation of two benzhydrazide and three S-ethylated pyridine-2-thiocarboxamides precursors. Reaction of these precursors produced three new 1,2,4-triazole- and one 1,3,4-oxadiazole -based ligands substituted with boronic acid pinacol ester groups. The boronic acid pinacol esters were then converted to boronic acids in two steps via potassium trifluoroborate intermediates. The boronic acid substituted ligands and their Ir(III) complexes were fully characterised using a range of techniques including X-ray crystallography in the case of the pyridyl-1,3,4-oxadiazole ligand and two of the Ir(III) complexes. The capacity of the synthesised Ir(III) complexes to form boronic acid cyclic esters with the simple sugars glucose and fructose was evaluated using high-resolution mass spectrometry (HRMS) and photoluminescence titration studies. These studies confirm that the Ir(III) complexes form adducts with both glucose and fructose, with increased levels of boronic acid cyclic esters being formed with fructose at higher pHs. Theoretical calculations were used to gain insight into the nature of the electronic transitions involved in the electronic absorption and emission spectra.

Introduction

Carbohydrates are components of many molecules that are fundamental to life such as DNA, RNA glycolipids and glycoproteins.[1] Carbohydrates are also important in disease diagnosis,[2] for example, unregulated levels of glucose in the blood are associated with the disease diabetes mellitus, which can result in serious complications such as heart disease, stroke and kidney damage.[3, 4] Additionally, glycated proteins are known to be potential markers for a number of diseases such as cancer, Alzheimer's disease and autoimmune disease. The ability to selectively detect these species would offer significant potential for the diagnosis and monitoring of the afore-mentioned conditions.[5]

A range of established methods are available to determine blood glucose concentrations, with many of these approaches utilizing enzymatic reactions (e.g. glucose oxidase) in combination with

electrochemical measurements.[6] An alternative enzyme-free approach for sensing or imaging carbohydrates utilizes boronic acid containing molecules and materials in combination with electrochemical, fluorescence or colorimetric measurements.[1, 5] Boronic acids are excellent receptors for carbohydrates (e.g. 1,2- or 1,3-diols) because the interaction is both rapid and reversible. Such species have also shown significant promise for sensing and imaging more complex carbohydrates and glycoproteins in cells.[7, 8]

In an effort to capitalise on these properties, an extensive range of luminescent organic molecules and materials that incorporate boronic acid groups have been prepared as potential agents for imaging and sensing carbohydrates.[5, 9] In general, these carbohydrate sensitive boronic acid-based probes signal the presence of carbohydrates such as glucose through either a change in their emission intensity or wavelength.[1, 5] Despite the large number of boronic acid containing probes that have been developed, relatively few metal-based luminophores have been reported as carbohydrate sensors.[10-16] The structures of two metal-based luminescent carbohydrate sensors are shown in Figure 1. The Re(I) complex **I**, showed pH dependent emission, as a result of a photoinduced electron transfer (PET) mechanism. Addition of glucose to the complex in methanol caused an increase in the fluorescence intensity, however the need for a pure organic solvent represents a significant drawback in terms of potential biological applications.[11] Addition of glucose to the Ru(II) complex **II** causes a quenching of the luminescent emission as a result of cleavage of the 2-methoxyphenylboronic acid unit from the complex.[13]

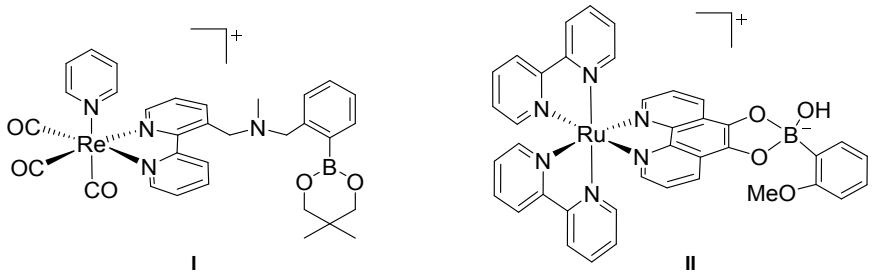

Figure 1. Examples of luminescent metal complex-based sensors for carbohydrates.

We have a long-standing interest in the development and characterisation of new luminescent Ru(II) and Ir(III) compounds, particularly of N-heterocyclic carbene ligands,[17-20] for application as electrochemiluminescent sensors[21] and as luminescent imaging agents.[22, 23] In the present paper, we report the synthesis of a series of three pyridyl-1,2,4-triazole and one pyridyl-1,3,4-oxadiazole ligands, which are substituted with boronic acid groups, together with their Ir(III) complexes. These complexes were designed as potential luminescent imaging agents for sugars and carbohydrates based on the well-known capacity of Lewis acidic boronic acids to form cyclic boronic acid esters with sugars and carbohydrates in aqueous solution. The propensity of the Ir(III) complexes to form adducts

View Article Online
DOI: 10.1039/D0DT02177F

with glucose and fructose esters was evaluated using high-resolution mass spectrometry (HRMS) and luminescence titration studies.

Results and Discussion

Ligand synthesis

A series of three 1,2,4-triazole-pyridine and one 1,3,4-oxadiazole -pyridine bidentate ligands bearing boronic acid groups were prepared using a modular synthetic scheme. The synthesis was initiated with the preparation of benzhydrazide **2a** and a benzhydrazide substituted with a boronic acid pinacol ester group at position 4 of the phenyl ring **2b** (Scheme 1), via a nucleophilic acyl substitution reaction between the ethyl ester compounds **1a** and **1b** with hydrazine hydrate.

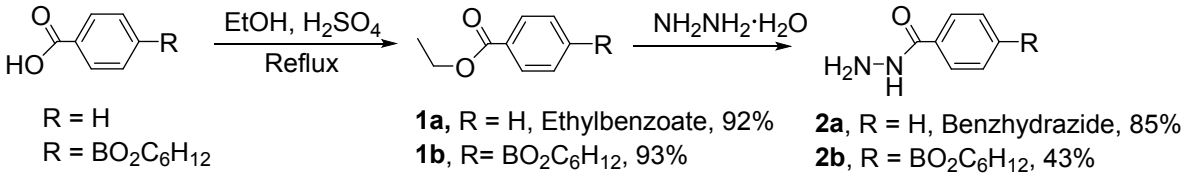

Scheme 1. Preparation of benzhydrazide compounds **2a** and **2b**.

To synthesise the desired 1,2,4-triazoles, the thioamides **3a-3c** (Scheme 2) were prepared utilizing a convenient synthetic methodology described by Brooker and co-workers.[24, 25] In this process the required *N*-substituted pyridine-2-thiocarboxamide compounds were prepared by heating 2-methylpyridine with the appropriate amine in the presence of sulfur and a catalytic amount of sodium sulfide (Scheme 2). To increase the reactivity of the thioamides **3a**, **3b** and **3c** towards nucleophilic attack from the hydrazides **2a** and **2b**, the thioamides were S-alkylated with bromoethane in the presence of sodium ethoxide yielding the S-ethylated products **4a**, **4b** and **4c** as orange oils (Scheme 2).[26] Due to their low stability and very unpleasant odour, these compounds were used promptly in the following reactions without additional purification.

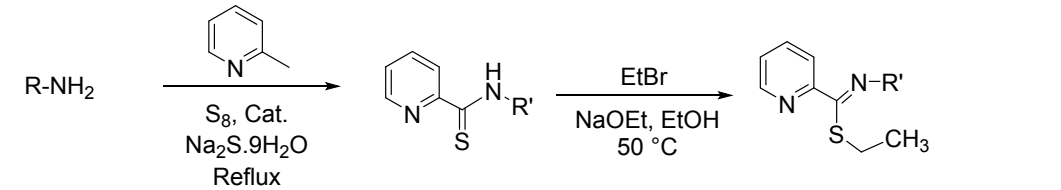

Scheme 2. Preparation of N-substituted pyridine-2-thiocarboxamides, **3a**, **3b** and **3c** and their S-ethylated congeners, **4a**, **4b** and **4c**.

Reaction of the S-ethylated thioamides **4a** and **4b** with hydrazide **2a** in 1-butanol generated the 1,2,4-triazoles **5a** and **5b** (Scheme 3). Similarly, compound **4c** was reacted with hydrazide **2b** yielding the triazole **5d**. ^{1}H NMR spectroscopy and TLC analysis of the crude product formed in the reaction between compounds **4b** and **2a** showed that two products were formed with one being the triazole **5b**. Triazole **5b** and the second product were separated by column chromatography and the unknown compound was subsequently identified as oxadiazole **5c** (Scheme 3). Compounds **5a**-**5d** were characterised using ^{1}H and ^{13}C NMR spectroscopy and these products showed the expected number of signals consistent with their structures, with each bearing boronic acid pinacol ester units. In the case of **5c**, an X-ray crystal structure was also obtained (see Structural Studies section).

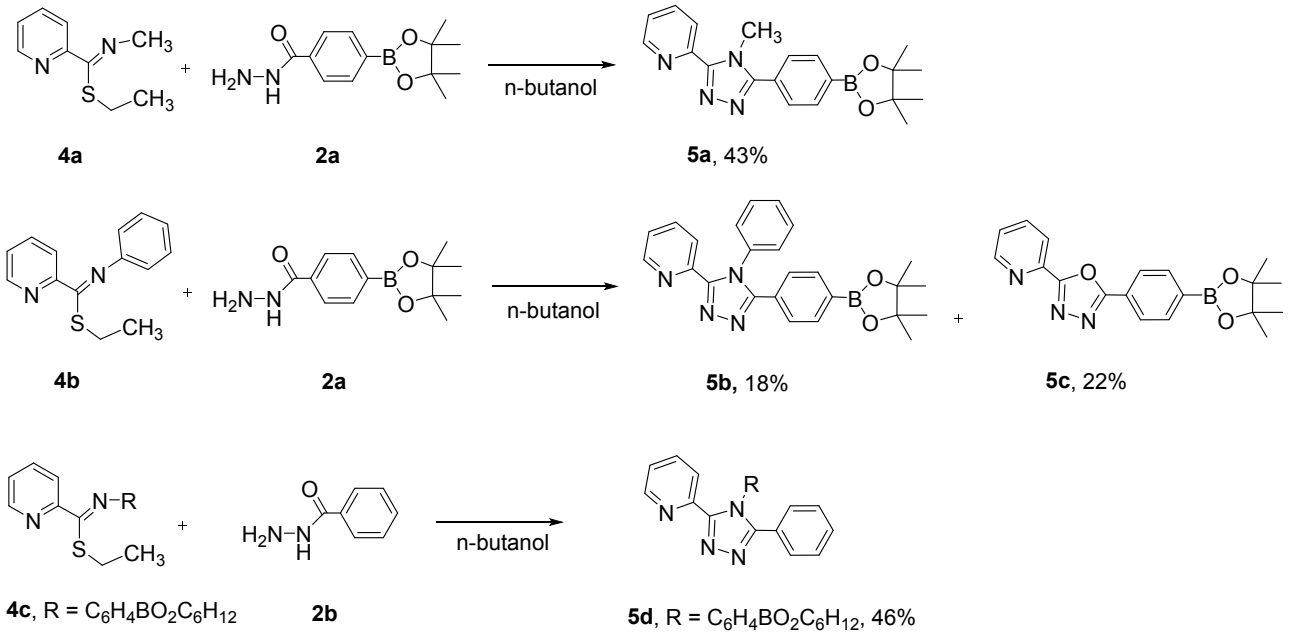

4a **2a** **5a**, 43%

4b **2a** **5b,** 18% **5c**, 22%

4c, R = $C_6H_4BO_2C_6H_{12}$ **2b** **5d**, R = $C_6H_4BO_2C_6H_{12}$, 46%

Scheme 3. Synthesis of 1,2,4-triazoles **5a**, **5b**, **5d** and 1,3,4-oxadiazole **5c**.

The formation of the oxadiazole product **5c** is of interest as 1,3,4-oxadiazoles have not been previously prepared via this synthetic approach. The abbreviated mechanism shown in Figure 2 is proposed to account for the formation of this product. Here cyclisation results from attack of the carbonyl oxygen of the hydrazide group on the carbon atom of the intermediate imine bond to form the oxadiazole ring and subsequent loss of aniline yields the final boronic ester functionalised compound **5c**.

View Article Online
DOI: 10.1039/D0DT02177F

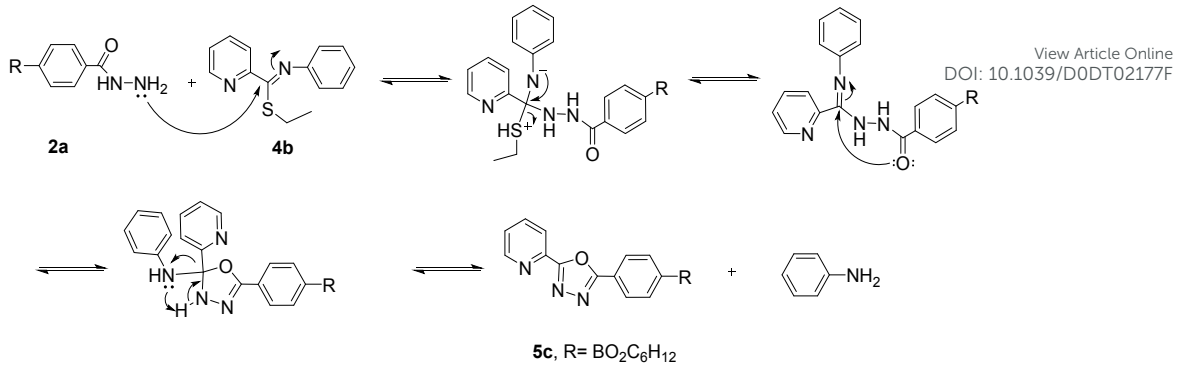

Figure 2. Abbreviated mechanism for the formation of oxadiazole compound **5c** from hydrazide **2a** and **4b**.

To prepare the desired ligands substituted with boronic acids, a two-step procedure was used to convert the boronic acid pinacol ester units of compounds **5a** - **5d**, to boronic acids. In this procedure the boronic acid pinacol ester was first converted to a trifluoroborate group (potassium salt) by treating **5a** – **5d** with a saturated solution of KHF_2 in methanol yielding compounds **6a** – **6d** (Scheme 4). The trifluoroborate group was then hydrolysed using LiOH and the desired 1,2,4-triazoles **7a**, **7b**, **7d**, and the oxadiazole **7c** functionalised with boronic acid groups were obtained in moderate yield (Scheme 4).[27] The ^{1}H and ^{13}C NMR spectra for **7a** – **7d** were consistent with the structures of these compounds. In each case the ^{1}H NMR spectra showed a broad peak in the region 8.15 – 8.33 ppm, corresponding to the $B(OH)_2$ group.

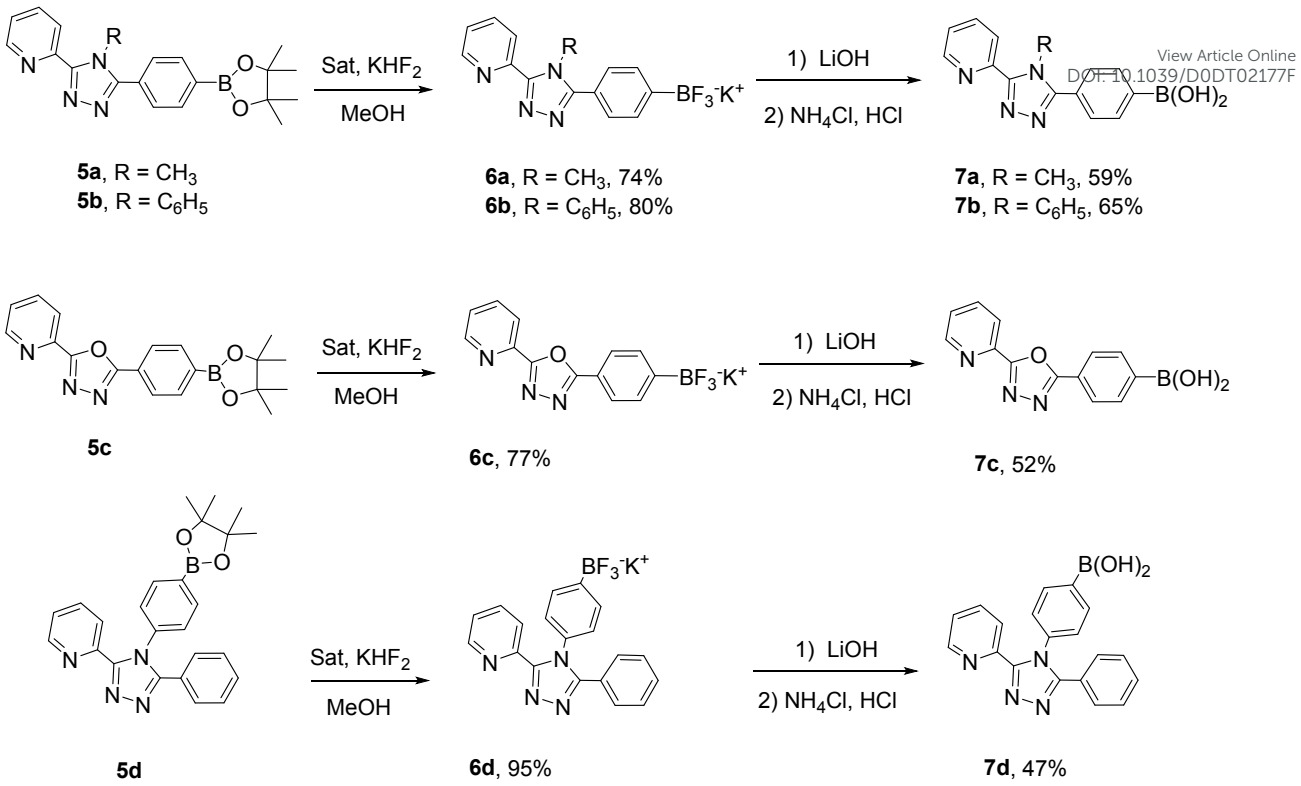

Scheme 4. Conversion of boronic ester groups of compounds **5a-5d** to boronic acid units via trifluoroborate intermediates.

Iridium complex synthesis

The cyclometalated Ir(III) complexes **8a** – **8d** were synthesised by the treatment of the chosen ligand (**7a** – **7d**) with the dimeric precursor complex $[Ir(ppy)_2Cl]_2$ (ppy = 2-phenylpyridine) in a mixture of dichloromethane and ethanol (Scheme 5). The complexes were obtained in moderate to good yields and were characterised by NMR spectroscopy and high-resolution mass spectrometry (HRMS) and in the case of complexes **8a** and **8c** by X-ray crystallography (see Structural Studies section). The high-resolution mass spectra of complexes **8a** – **8d** showed one major peak located at *m*/*z* = 781.2083, 843.2249, 768.1771, and 843.2245 respectively (Figure S7-S10, ESI) and in each case, these peaks correspond to the exact mass of complexes (calculated masses: 781.2074, 843.2231, 768.1758, and 843.2231). The ^{1}H NMR spectra for the complexes show a broad downfield shifted peak at 8.41, 8.26, 8.40, and 8.46 ppm for each of the complexes **8a** – **8d** corresponding to the boronic acid group.[28]

View Article Online
DOI: 10.1039/D0DT02177F

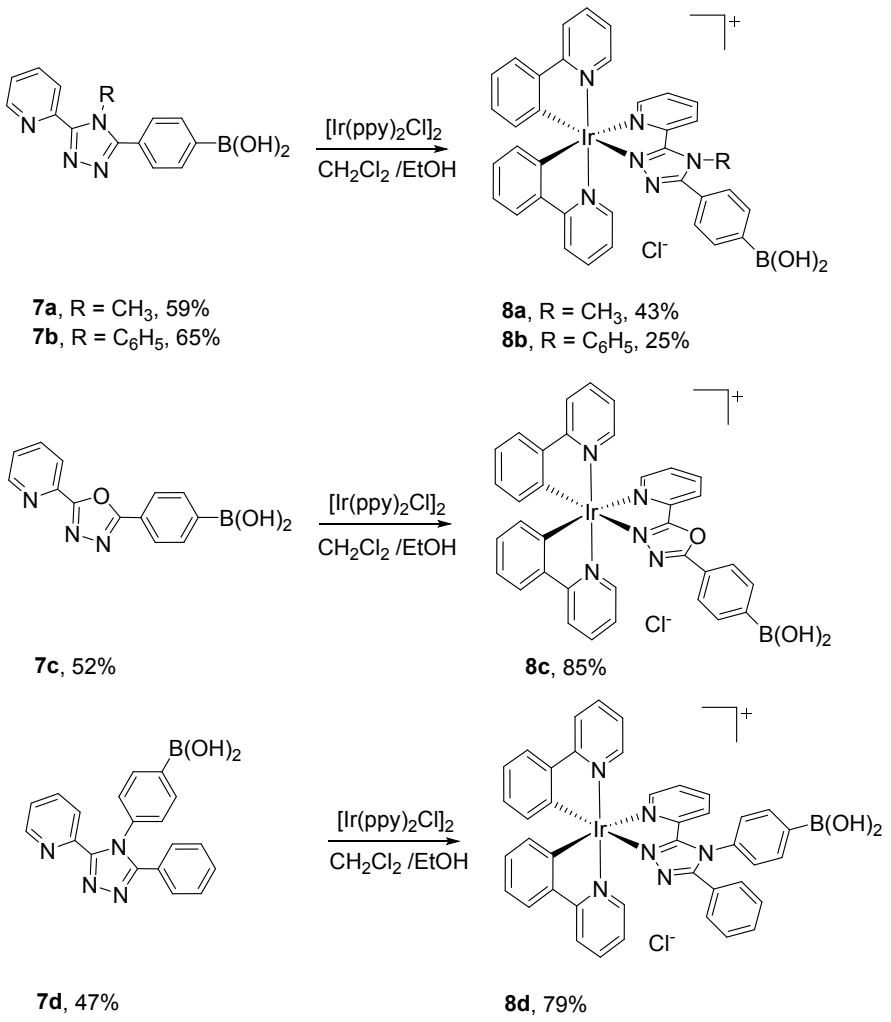

Scheme 5. Synthesis of Ir(III) complexes **8a** – **8d** from boronic acid substituted ligands **7a** – **7d**.

Structural Studies

Single crystals suitable for X-ray diffraction studies were obtained for the 1,3,4-oxadiazole compound **5c** and the Ir(III) complexes **8a** and **8c**, and the structures of these compounds are shown in Figure 3. The X-ray crystal structure of **5c** confirms that a 1,3,4-oxadiazole ring was formed and that this is coupled to the pyridyl group and the phenylboronic acid pinacol ester unit at positions 2 and 5 respectively. The oxadiazole ring C-O bond distances are similar (C1-O1 = 1.3657(16) Å and C2-O1 = 1.3627(15) Å). The Ir(III) complex structures (**8a** and **8c**) display slightly distorted octahedral coordination geometries for the Ir(III) metal centres with two cyclometallating 2-(phenyl)pyridine ligands and the 1,2,4-triazole-pyridine ligands. In each case, the pyridyl groups of the 2-(phenyl)pyridine ligands adopt mutually *trans* dispositions respectively. The metal-ligand bond distances for these complexes are given in Table 1 and the Ir–$N_{triazole}$ bond distance for compounds **8a** is slightly shorter (2.095(3) Å) than the Ir–$N_{oxadiazole}$ bond distance (2.152(2) Å) found for compound **8c**. These bond distances are similar to those reported previously for related Ir(III) complexes. For example, the Ir–$N_{triazole}$ bond distance for the Ir(III) complex of the ligand 2-[3-

(trifluoromethyl)-1,2,4-triazol-5-yl]pyridine is 2.116 Å,[29] while the Ir–$N_{oxadiazole}$ bond distance for the Ir(III) complex of 2-(5-phenyl-1,3,4-oxadiazol-2-yl)pyridine is 2.158 Å.[30] In the case of compound **8a**, hydrogen bonding interactions are evident, with the O-H groups of the boronic acid being hydrogen bonded to the chloride anion and a water molecule (Figure 3b). In the case of the oxadiazole complex **8c**, the X-ray quality crystals were obtained from a solution of the complex in methanol and as a result of this choice of solvent the boronic acid group has been converted to a monomethyl boronic acid ester. The remaining boronic acid O-H group is hydrogen bonded to the chloride anion with the distance (O2-Cl1) being 3.062 Å.

Table 1. Selected bond distances (Å) from the X-ray structures of iridium(III) complexes **8a** and **8c**.

Bond	**8a**	**8c**
Ir-N1	2.095(3)	2.152(2)
Ir-N3	2.173(3)	2.193(2)
Ir-N4	2.035(4)	2.050(2)
Ir-N5	2.049(3)	2.053(2)
Ir-C14	2.013(4)	2.009(2)
Ir-C25	2.014(4)	2.011(2)

View Article Online
DOI: 10.1039/D0DT02177F

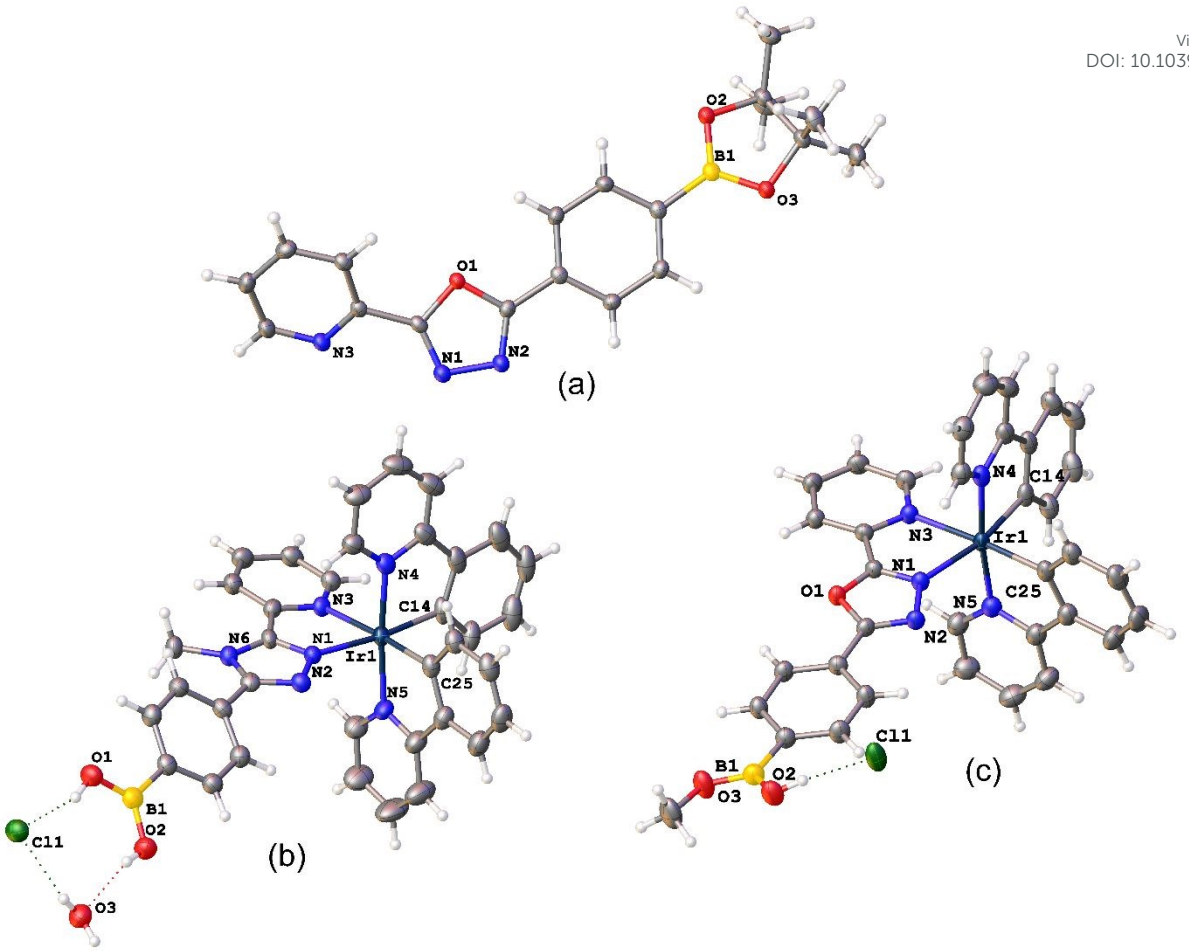

Figure 3. Single crystal diffraction structures of the (a) 1,3,4-oxadiazole compound **5c** and the Ir(III) complex (b) **8a** and (c) **8c**. Solvent of crystallization omitted for clarity (except for **8a**) and ellipsoids are shown 40% probability.

Photoluminescence studies

The photophysical properties of Ir(III) complexes **8a-8d** were evaluated and the UV-visible spectra for these complexes are shown in Figure 4a. On the basis of theoretical studies (see Theoretical Calculations section) and comparison with previously reported Ir(III) complexes[31, 32] the intense absorption bands at shorter wavelength (~260 nm) can be assigned to ligand-to-ligand charge transfer (LLCT), while, the less intense bands at lower energies (>300 nm) are best assigned to admixed ligand centred (LC) and metal to ligand charge transfer (MLCT) transitions. The absorption spectrum for complex **8c** (oxadiazole ligand) is different to the other complexes with a second prominent absorption band centred at ~300 nm. The photoluminescence spectra for complexes **8a-8d** are shown in Figure 4b. The emission spectra are similar for all complexes with one broad emission band centred at ~590 nm (λ_{ex} = 346 nm). Such broad unstructured emission is consistent with a MLCT or LLCT excited state, as predicted by the theoretical studies *vide infra*.

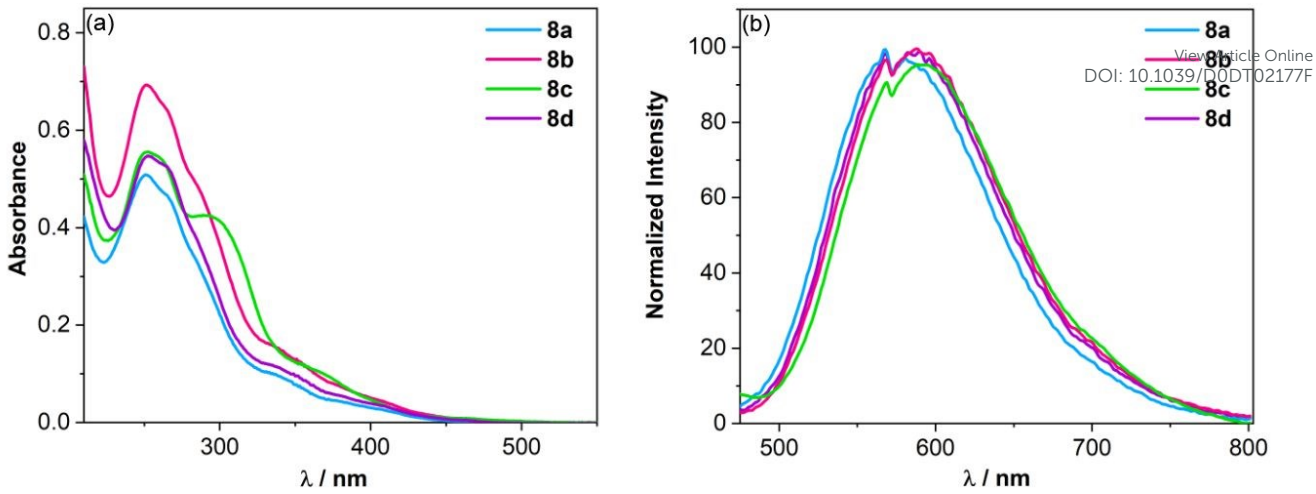

Figure 4. (a) The UV-Vis absorption spectra and (b) photoluminescence emission spectra for complexes **8a** (blue), **8b** (pink), **8c** (green) and **8d** (purple). The concentration in each case is 20 μM, in aqueous *tris*-buffered solutions at pH = 9. The spike at 569 nm is an instrumental artefact due to the switch between diffraction gratings at that wavelength.

Mass Spectrometric Boronic acid Sugar Binding studies

The boronic acid substituted complexes **8a-8d** were prepared as potential luminescent sensors for carbohydrates[33-35] and in an initial study, the capacity of complex **8d** to bind to the sugars fructose and glucose was evaluated using high-resolution mass spectrometry (HRMS). Glucose and fructose were chosen for these studies due to their significant biological importance and because boronic acid-based sensors often display different binding affinities for these sugars,[5] thereby allowing for an initial assessment of the sensitivity and selectivity of these complexes. These initial measurements were made at pH=7 and 9 as it has been shown previously that the capacity of boronic acid containing compounds to bind carbohydrates via cyclic boronic acid ester formation is pH dependent, with the tetrahedral boronate species formed at higher pH values (>9) facilitating boronic ester formation when compared to the corresponding boronic acids.[34, 36] The HRMS spectra for complex **8d** in the presence of fructose at pH 7 and 9 are shown Figures 5a and b respectively, while the spectra obtained for **8d** in the presence of glucose at pH 7 and 9 are shown in Figures 5c and d, respectively.

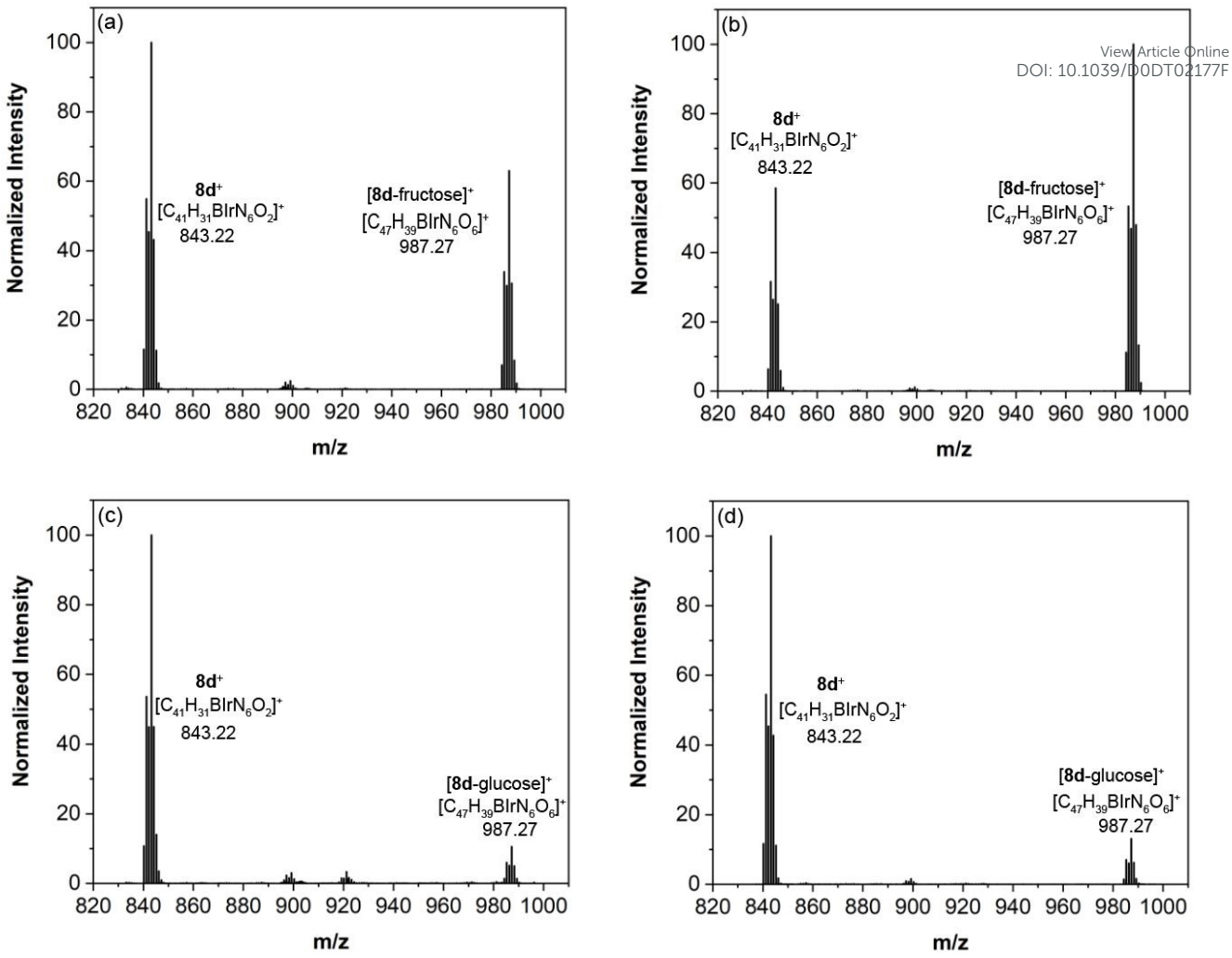

Figure 5. High resolution mass spectra recorded for complex **8d** in the presence of (a) fructose (pH=7), (b) fructose (pH =9), (c) glucose (pH=7) and (d) glucose (pH=9). [**8d**] = 1.48×10^{-4} M, [sugar] = 1.48×10^{-3} M.

The spectra shown in Figure 5 for compound **8d** in the presence of fructose (a, pH=7 and b, pH=9) and glucose (c, pH=7 and d, pH=9) show two main peaks, the first at m/z = 843.22 corresponds to the complex cation while the second at m/z = 987.27 corresponds to the mass of the cyclic boronic acid esters formed from these sugars (both fructose and glucose have the same molecular weight: 180.16 g/mol). The spectra obtained for **8d** in the presence of fructose (Figure 5a and b) show a significantly more intense peak is obtained for the boronic acid cyclic ester for this sugar when compared to glucose. This result indicates that the complex forms an adduct with fructose more readily than with glucose and this is consistent with a number of previous studies, which show that boronic acid sensors more readily form boronic acid esters with fructose[33, 34, 37] than glucose.[38] The spectra shown in Figure 5 also demonstrate that the solution pH also has a strong effect on sugar-adduct formation, with higher levels of the sugar adducts formed at elevated pH (e.g. pH=9). Again, this finding is consistent with previous studies that show that the boronate anion (formed at higher pH when the Lewis acidic

boronic acid reacts with hydroxide anions) reacts more readily with diols to form boronic acid cyclic esters.[34, 36]

View Article Online
DOI: 10.1039/D0DT02177F

Luminescent Titration Sugar Binding Studies

Luminescent titration studies were conducted for the Ir(III) complexes with increasing ratios of the sugars fructose and glucose. For complexes **8a-8c** these studies were conducted at pH=9, while for **8d** the studies were conducted at pH = 7 and 9. The results for complex **8d** are shown in Figure 6 while the results for complexes **8a-8c** are given in Figure S11 (ESI). Complex **8d** exhibits a broad emission centred at ~590 nm (λ_{ex} = 346 nm) in *tris* buffer (20 mM) at pH = 7 and 9. The addition of an increasing molar ratio of fructose (0 → 2 molar equivalents) to a solution of **8d** at pH = 7 (Figure 6a) resulted in a modest 9% quenching of the luminescent emission band at 590 nm. In contrast, when the same additions were made to **8d** at pH = 9 (Figure 6b), a significantly greater quenching (39%) of the emission band was observed. As was also seen in the mass spectrometric studies, it is apparent that lower levels of the boronic acid cyclic ester is formed between complex **8d** and glucose than for fructose. The addition of glucose (0 → 2 molar equivalents) to **8d** at pH = 7 and 9 resulted in moderate quenching of the emission band with values of 11% and 14% respectively. Similar results are observed for the UV-visible absorption spectra for complex **8d**. A decrease in the absorptivity of the complex is observed (particularly for the intense band centred at ~260 nm) with the addition of fructose (Figure S12a and b) and glucose (Figure S12c and d, ESI), with these effects mirroring the changes seen in the emission spectra. The titration results for complexes **8a-8c** (Figure S11, ESI) show only relatively low levels of quenching of the emission spectra in the presence of either fructose or glucose.

These results suggest that the position of the boronic acid group is critical to the ability of these compounds to act as luminescent receptors for sugars. When the phenyl ring bearing the boronic acid group is coupled to N4 of the triazole ring (as is the case for **8d**) a significant sensitivity of the emission intensity to the presence of fructose (at pH=9) is observed. In contrast, for complexes where the phenyl ring is coupled to a carbon atom (C3 for the 1,2,4-triazoles or C2 for the oxadiazole) a considerably lower sensitivity to the sugars is observed. Although the mechanism of fluorescence quenching for these complexes has not been investigated, similar results have been previously reported for boronic acid-based carbohydrate sensors.[1] For example, in an early study by Yoon and Czarnik, an anthracene boronic acid-based sensor showed fluorescence quenching, with increased quenching levels observed at higher carbohydrate concentrations and pH values as a result of an excited state internal charge transfer (ICT) process.[33] These results are similar to those obtained in the present study and were attributed to the increased propensity of the boronic acid cyclic ester to form the corresponding borate anions compared to the boronic acid. With the sp^3 hybridised anionic

borate species being less fluorescent than the sp^2 hybridised boronic acid or cyclic boronic acid ester forms.[33]

View Article Online
DOI: 10.1039/D0DT02177F

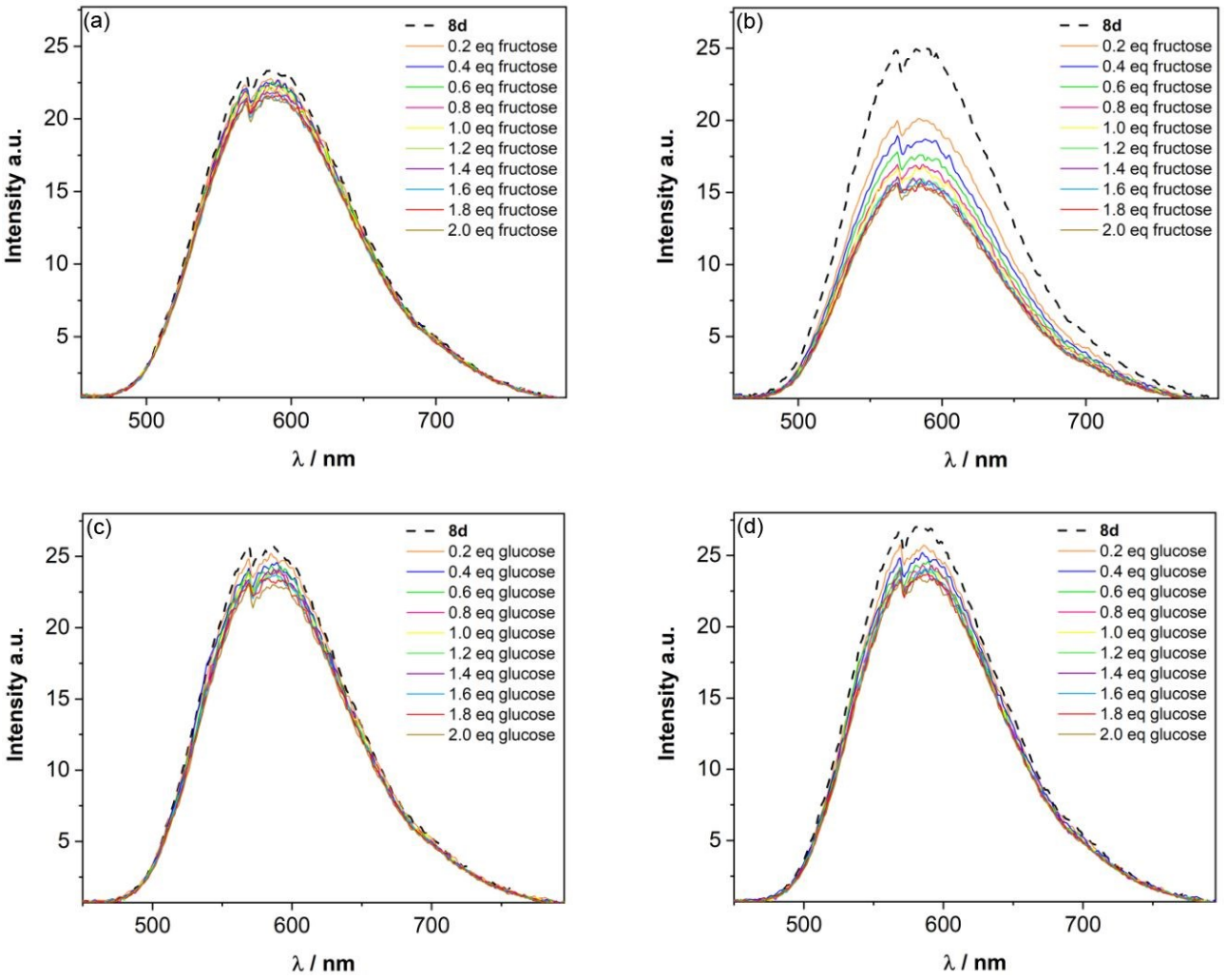

Figure 6. Luminescent titration of compound **8d** with the sugars (a) fructose pH = 7; (b) fructose pH = 9; (c) glucose, pH = 7 and (d) glucose pH = 9. [Complex] = 20 μM, [*tris* buffer] = 2.0 mM. The spike at 569 nm is an instrumental artefact due to the switch between diffraction gratings at that wavelength.

Theoretical Studies

The optimized geometries of complexes **8a-8d** yield similar Ir-C and Ir-N bond distances (Table 2), with bond distances for compounds **8a** and **8c** being in good agreement with the X-ray structures (Table 1).

View Article Online
DOI: 10.1039/D0DT02177F

Table 2. mPW1PW91/def2-SVP calculated bond distances for Ir-C and Ir-N bond for complexes **8a-8d** (Å).

Bond	**8a**	**8b**	**8c**	**8d**
Ir-N1	2.153	2.150	2.168	2.150
Ir-N3	2.213	2.218	2.237	2.218
Ir-N4	2.062	2.066	2.065	2.065
Ir-N5	2.063	2.065	2.065	2.065
Ir-C14	2.012	2.013	2.008	2.013
Ir-C25	2.008	2.008	2.007	2.007

Plots of the frontier molecular orbitals (MOs) for **8a-8d** are shown in Figure 7. For each complex, the HOMO is centred on the metal and phenylpyridine (C^N) ligands, while the LUMO (and LUMO+1) is located on the auxiliary N^N ligand. For compounds **8a-8c** there is a non-negligible contribution to the LUMO from the phenyl group of the boronic acid moiety, which is absent in **8d**.

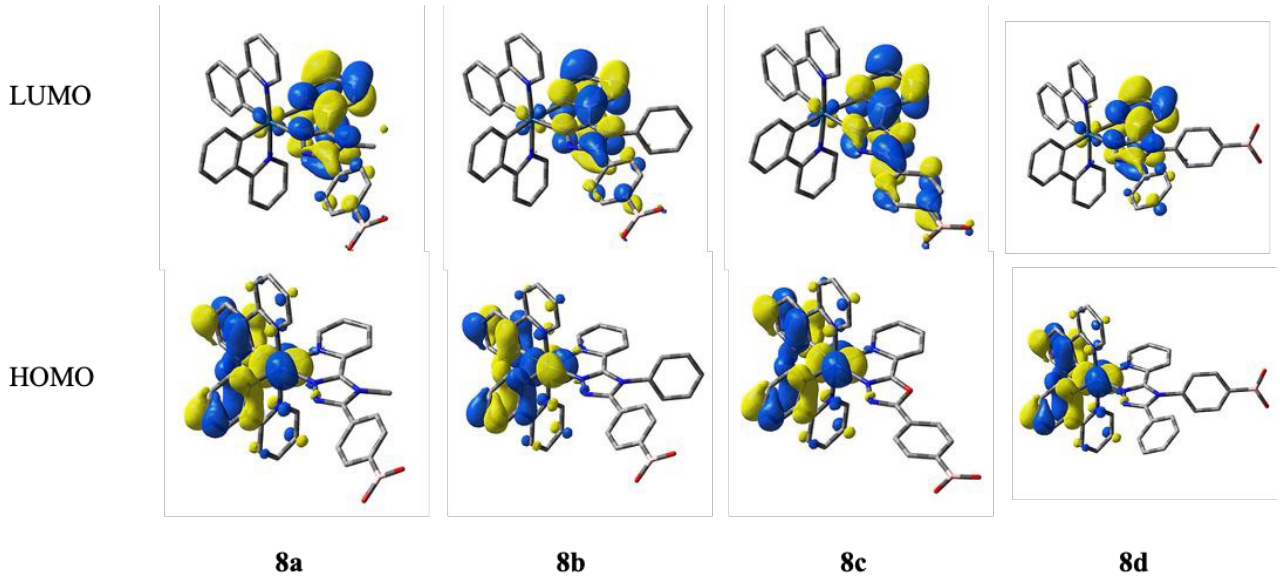

Figure 7. Plots of BP86/def2-TZVP calculated molecular orbitals of complexes **8a-8d**.

Analysis of the frontier MOs was carried out to characterise orbitals according to their Mulliken population from molecular fragments of the metal, N^N coordinated, and C^N coordinated ligands, with results for complexes **8a-8d** plotted in Figure 8. In each case, the HOMO includes a large (~45%) contribution from the iridium *d*-orbitals, with only a minor contribution of 2-3% from the N^N ligands (either pyridyl-1,2,4-triazole for **8a**, **8b** and **8d** or pyridyl-1,3,4-oxadiazole for **8c**). The largest contribution to the HOMO for these complexes is from the 2-phenylpyridine ligands (~48%). The LUMO is similar in nature for all four complexes, with the metal only contributing 2-3%, while the

dominant contribution (95-97%) comes from the triazole or oxadiazole N^N ligands. There is a negligible contribution from the boronic acid moiety to either the HOMO or LUMO of all four complexes.

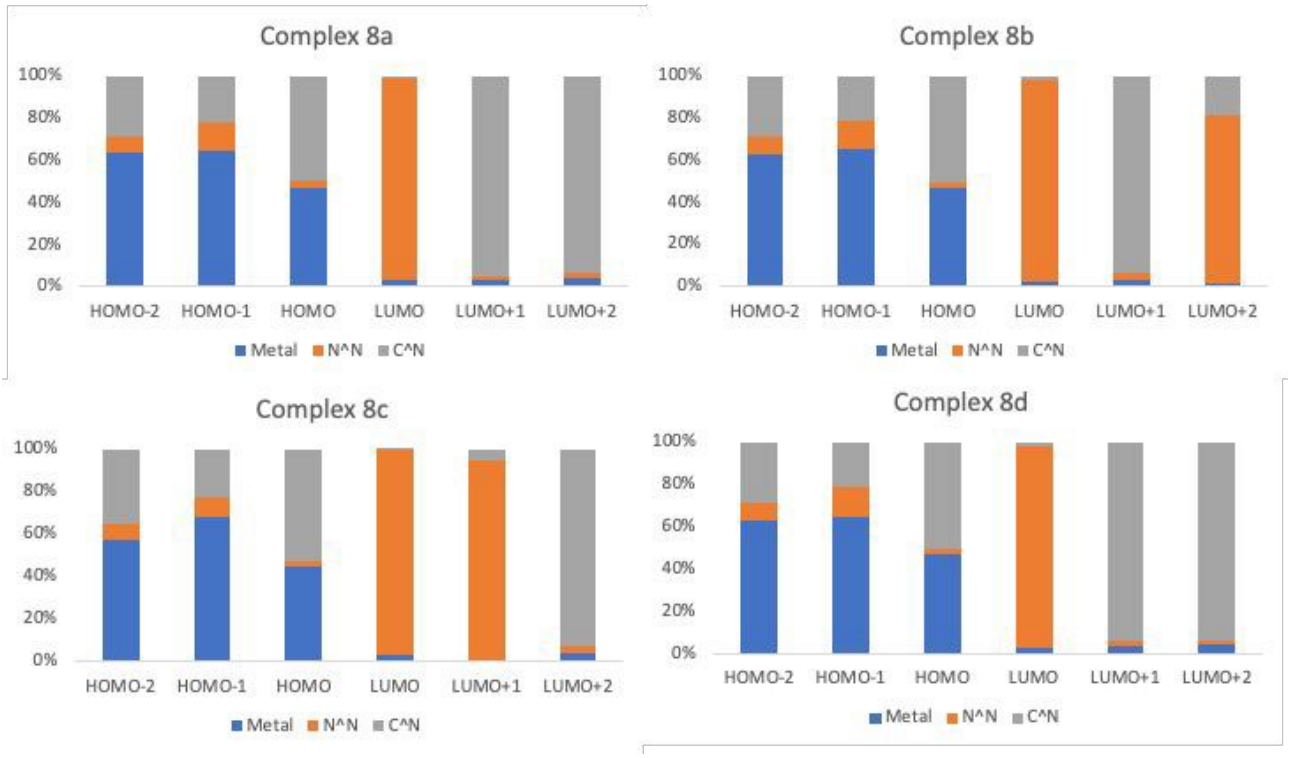

Figure 8. BP86/def2-TZVP calculated Mulliken populations of the frontier MOs of complexes **8a-8d**.

Time-dependent density-functional theory (TD-DFT) calculations were carried out to elucidate the nature of the transitions in the absorbance profiles (Table 3). For all complexes, the higher energy transitions (λ_{abs} < 300 nm) are identified as predominantly ligand-to-ligand charge transfer (LLCT) transitions. Transitions occurring within the range 300-360 nm can be predominantly characterised as metal-to-ligand charge transfer (MLCT) and metal-ligand-to-ligand charge transfer transitions (MLLCT) associated with excitation from the HOMO. The most intense transitions are typically the HOMO-LUMO and HOMO-LUMO+1, although here **8c** appears to be different with the HOMO-LUMO oscillator strength being negligible while the HOMO-2 to LUMO transition has appreciable oscillator strength. These TD-DFT results rationalise the different absorbance spectrum observed for **8c** in comparison with the other complexes.

View Article Online
DOI: 10.1039/D0DT02177F

Table 3. ωB97XD/def2-TZVP calculated absorbance wavelength (nm), oscillator strength, and dominant contribution of the first three transitions of complexes **8a**-**8d**.

	Excitation	Wavelength	Oscillator Strength	Contributions
8a	1	331.88	0.079	54.0% HOMO → LUMO+1
	2	327.05	0.081	51.2% HOMO → LUMO
	3	320.69	0.006	80.1% HOMO → LUMO+2
8b	1	329.48	0.038	70.3% HOMO → LUMO
	2	328.29	0.117	73.6% HOMO → LUMO+1
	3	319.68	0.006	81.1% HOMO → LUMO+2
8c	1	351.49	0.003	77.3% HOMO → LUMO
	2	326.29	0.158	80.1% HOMO → LUMO+1
	3	318.38	0.083	44.6% HOMO-2 → LUMO
8d	1	329.20	0.056	65.1% HOMO → LUMO
	2	328.36	0.097	66.2% HOMO → LUMO+1
	3	319.85	0.006	81.6% HOMO → LUMO+2

Conclusion

A modular synthetic procedure has been developed for the generation of bidentate 1,2,4-triazole- and 1,3,4-oxadiazole -based ligands bearing boronic acid groups. The developed synthesis is convergent and benzhydrazide and pyridine-2-thiocarboxamide precursors substituted with boronic acid groups protected as pinacol esters were initially prepared. This approach allowed for the introduction of the boronic acid units at two different positions on the final ligand molecules. The Ir(III) complexes of the synthesised triazole and oxadiazole ligands were synthesised in a straight forward manner by reaction of the precursor complex $[Ir(ppy)_2]_2$ with the chosen ligand.

This series of Ir(III) complexes were prepared as potential luminescent sensors for carbohyrates as, although there has been great interest in boronic acid-based carbohydrate probes there remains very few examples which incorporate inorganic luminophores. Luminescent inorganic molecules offer several potential advantages over organic probes for biological applications, such as large Stokes shifts, long luminescent lifetimes and resistance to photobleaching. The luminescent properties of the prepared complexes were investigated, and the complexes were emissive at ~590 nm. Theoretical computational studies showed that the HOMO for this series of complexes is primarily centred on the iridium *d*-orbitals and 2-phenylpyridine ligands while the LUMO is predominantly on the N^N ligands (either pyridyl-1,2,4-triazole or pyridyl-1,3,4-oxadiazole).

The capacity of the complexes to form cyclic boronic acid esters with the sugars glucose and fructose was evaluated using both high resolution mass spectrometry (in the case of complex **8d**) and luminescence titration studies. The results of these studies show that the complexes displayed increased levels of cyclic boronic ester formation with fructose when compared to glucose. Higher binding affinities for fructose compared to glucose for monoboronic acids such as compounds **8a**-**8d**, has been noted previously and is believed to result from fructose adopting a relatively high concentration of the β-D-fructofuranose form in solution,[39, 40] which contains a pair of hydroxyl groups that are ideally oriented for boronic acid binding.[41] In addition, a clear dependence on solution pH was seen for sugar-adduct formation, with adducts formed more readily at higher pH (e.g. pH=9). This finding is likely to result from the boronate anion (formed at higher pH when the Lewis acidic boronic acid reacts with hydroxide anions) reacting more readily with diols, to form the boronate cyclic ester.

On the basis of results for previously reported mono-boronic acid sensors, the new Ir(III)-based complexes described here are not expected to display significant selectivity for other more complex carbohydrates such as N-acetyl-substituted sugars or glycoproteins/glycolipids. The development of selective boronic acid-based sensors has been a field of significant interest and a raft of compounds based on organic luminophores have been evaluated.[1] Diboronic acid-based sensors, which provide a selective recognition site for carbohydrates have received considerable attention. For example compound **9** was designed based on a rigid scaffold to specifically complex α-D-glucopyranose at the 1,2 and 4,6 positions.[42]

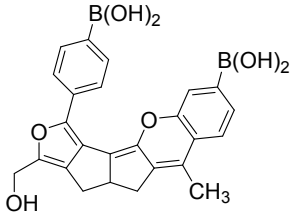

9

Figure 9. Structure of diboronic acid-based sensor (**9**) designed to specifically complex α-D-glucopyranose.[42]

Similar approaches have also been investigated for the selective recognition of more complex carbohydrates and a diboronic acid-functionalized peptide receptor has been reported for the recognition of cell surface glycans such as the cancer-associated glycan sialyl Lewis X.[43]

Although experimental results show that compounds **8a** - **8d** do form the desired adducts with the sugars glucose and fructose, only low to moderate levels of photoluminescence quenching were observed for even the most active complex **8d**. These studies suggest that the influence of sugar

binding on luminescence depends on proximity to a frontier orbital. Therefore, we are currently developing a new class of sensors where the boronic acid group is placed closer to the metal atom or located on the 2-phenylpyridine ligands. Incorporation of the boronic acid groups on the 2-phenylpyridine ligand will allow for Ir(III) complexes to be prepared bearing two boronic acid groups, so as to provide increased selective recognition for carbohydrates.

Experimental Details

General Procedures

All reagents were purchased from Sigma Aldrich, Alfa Aesar or Precious Metals Online and were used without further purification. NMR spectra were recorded on either a Bruker Avance ARX-400 (400.13 MHz for 1H, 100.61 MHz for 13C), or a Bruker Avance ARX-500 (500.13 MHz for ^{1}H, 125.77 MHz for ^{13}C) spectrometer and were internally referenced to solvent resonances. High-resolution mass spectra were obtained using an Agilent 6530 QTOF LC/MS mass spectrometer fitted with an Agilent electrospray ion (ESI) source. UV-visible spectra were recorded using an Agilent Technologies Cary 300 UV-visible spectrophotometer using quartz cuvettes (1 cm). Fluorescence spectra were recorded on a Varian Cary Eclipse spectrofluorimeter (5 nm bandpass, 1 nm data interval, PMT voltage: 600 V) using quartz cuvettes (1 cm).

X-ray Crystallography

Single crystals of ligand **7c** and complexes **8a** and **8d** suitable for X-ray diffraction studies were grown by slow evaporation in dichloromethane solutions of these complexes. Crystallographic data for all structures determined are given in Table S1 (ESI). For all samples, crystals were removed from the crystallisation vial and immediately coated with Paratone oil on a glass slide. A suitable crystal was mounted in Paratone oil on a glass fibre and cooled rapidly to 128 K (**7c**) or 116 K (**8a**) or 150 K (**8d**) in a stream of cold N_2 using an Oxford low-temperature device. Diffraction data were measured using an Oxford Gemini diffractometer mounted with Mo-Kα λ = 0.71073 Å and Cu-Kα λ = 1.54184 Å. Data were reduced and corrected for absorption using the CrysAlis Pro program.[44] The SHELXL2013-2[45] program was used to solve the structures with Direct Methods, with refinement by the Full-Matrix Least-Squares refinement techniques on F2. The non-hydrogen atoms were refined anisotropically and hydrogen atoms were placed geometrically and refined using the riding model. Coordinates and anisotropic thermal parameters of all non-hydrogen atoms were refined. All calculations were carried out using the program Olex2.[46] Further XRD details are provided in the Electronic Supplementary Information. CCDC 2005921-2005923 contains the supplementary crystallographic data for this paper. These data can be obtained free of charge from The Cambridge Crystallographic Data Centre via https://www.ccdc.cam.ac.uk/structures/

View Article Online
DOI: 10.1039/D0DT02177F

High resolution mass spectrometric sugar-binding studies

To 1 mL of an aqueous stock solution of complex of **8d** (1.48×10^{-4} M) was added 1 mL of either fructose (1.48×10^{-3} M) or 1 mL of glucose (1.48×10^{-3} M) solutions. The pH of the solutions (either 7 or 9) were adjusted by adding aliquots of an aqueous NaOH (0.01 M) solution. Mass spectra were recorded 3 h after mixing.

Photoluminescence sugar-binding studies

Stock solution of Ir(III) complexes **8a-8d** (1 mM) were prepared in methanol and 40 μL of the chosen stock was diluted with 2 mL of *tris* buffer (20 mM) and adjusted to either pH 7 or 9, giving a final complex concentration of 20 μM. The titration was carried out with additions of either fructose or glucose stock solutions (2 μL, 4 mM) prepared in *tris* buffer at the appropriate pH. The UV-visible absorption and luminescence spectra were recorded 10 minutes after mixing. The excitation wavelength used in the photoluminescence studies was 335 nm.

Computational Methods

DFT calculations were carried out within the Gaussian 16 suite of programs.[47] Ground state geometries were optimized with the mPW1PW91 functional[48] in conjunction with the def2-SVP basis set.[49, 50] Stationary points were characterized as minima through analytical frequency calculations at the same level of theory. All structures are minima with no imaginary frequencies. Molecular orbital (MO) analysis was performed using the def2-TZVP basis set and core potential,[49, 50] combined with the BP86 functional.[51, 52] TD-DFT calculations were performed using the ωB97XD functional[53] and def2-SVP basis set. All calculations included the use of an implicit solvent model of acetonitrile and utilized the polarizable continuum model (PCM) self-consistent reaction field (SCRF)[54] together with Truhlar's SMD solvent model.[55]

Synthesis

3c. A mixture of 4-aminophenylboronic acid pinacol ester (5 g, 22.8 mmol), sulfur (15 g, 468 mmol) and $Na_2S.9H_2O$ (2 g) in 2-methylpyridine (60 mL) was heated at reflux for 24 h. The mixture was then cooled to RT and the volatiles were evaporated under reduced pressure. The resulting dark brown liquid was purified on silica with hexane and ethyl acetate 4:1 as the eluent. Compound **3c** was obtained as a brown crystalline solid (yield 6.6 g, 85%). ^{1}H NMR (500 MHz, $CDCl_3$): δ =1.36 (s, 12 H, C*H*$_3$), 7.48 (t, $^3J_{HH}$ = 6.15 Hz, 1 H, Py*H*), 7.87-7.92 (m, 3 H), 8.12-8.14 (m, 2 H, Ph*H*), 8.56 (d, $^3J_{HH}$ = 4.69 Hz, 1 H, Py*H*), 8.80 (d, $^3J_{HH}$ = 8.03 Hz, 1 H, Py*H*), 12.14 (br. s, 1 H, CSN*H*) ppm. ^{13}C

NMR (500 MHz, $CDCl_3$): δ = 25.1 (4-*C*H_3), 84.1 (2 C, *C*q), 121.7 (Ph*C*), 125.0 (Py*C*), 126.3(Py*C*), 135.8 (Ph*C*), 137.7 (Py*C*), 141.4 (Ph*C*), 146.7 (Py*C*), 151.7 (Py*C*), 188.0 (*C*SNH) ppm.

4a. To a solution of NaOEt (prepared by dissolving sodium (0.6 g, 26.2 mmol) in dry ethanol (100 mL) was added compound **3a** (3.32 g, 21.81 mmol) and the reaction mixture was stirred at RT for 30 minutes. Bromoethane (2.85 g, 26.17 mmol) was then added to the orange solution, and the reaction mixture was heated at 50 °C for 24 h during which time a precipitate of NaBr formed. After cooling, the mixture was filtered through a plug of Celite and the volatiles were evaporated from the filtrate under reduced pressure. The orange liquid residue was dissolved in dichloromethane (60 mL) and the mixture was washed with water, brine and finally 1 M Na_2CO_3 and dried with Na_2SO_4. Evaporation of the volatiles under reduced pressure gave **4a** as an orange oil (yield 3.33 g, 85%). This material was unstable and attempts to purify it on silica were unsuccessful and it was utilised in following reactions without purification or characterisation.

4b. This compound was prepared as described for **4a** from NaOEt (prepared by dissolving sodium (0.59 g, 25.76 mmol) in ethanol (100 mL), **3b** (4.6 g, 21.46 mmol) and bromoethane (2.81 g, 25.76 mmol) and was obtained as an orange oil (yield 4.94 g, 95%).

4c. This compound was prepared as described for **4a** from NaOEt (prepared by dissolving sodium (0.07 g, 3.17 mmol) in anhydrous ethanol (30 mL), **3c** (0.9 g, 2.65 mmol) and bromoethane (0.35 g, 3.17 mmol) and was obtained as an orange oil (yield 0.94 g, 96%).

5a. A mixture of **4a** (0.70 g, 3.88 mmol) and **2a** (1.22 g, 4.65 mmol) in 1-butanol (20 mL) was heated at reflux for 72 h. On cooling, the product crystallized from the reaction mixture. Diethyl ether (10 mL) was added and the solid was collected yielding compound **5a** as a colourless solid. (yield 0.60 g, 43%). ^{1}H NMR (500 MHz, $CDCl_3$): δ = 1.38 (s, 12 H, C*H*$_3$), 4.07 (s, 3 H, C*H*$_3$),7.36 (t, $^3J_{HH}$ = 6.26 Hz, 1 H, Py*H*), 7.71-7.73 (m, 2 H, Ph*H*) , 7.85 (t, $^3J_{HH}$ = 7.74 Hz, 1 H, Py*H*), 7.96-7.98 (m, 2 H, Ph*H*), 8.35 (d, $^3J_{HH}$ = 7.95 Hz, 1 H, Py*H*), 8.68 (d, $^3J_{HH}$ = 4.84 Hz, 1 H, Py*H*) ppm. ^{13}C NMR (500 MHz, $CDCl_3$): δ = 25.11 (4-*C*H_3), 34.5 (*C*H_3), 84.4 (2 C, *C*q), 124.2 (Py*C*), 124.3 (Py*C*), 128.6 (Ph*C*), 129.8 (Ph*C*), 135.3 (Ph*C*), 137.2 (Py*C*), 148.3 (Py*C*), 149.0 (Py*C*), 153.7 (Tz*C*), 157.0 (Tz*C*) ppm.

5b and **5c.** A mixture of **4b** (0.92 g, 3.8 mmol) and **2a** (0.83 g, 3.17 mmol) in 1-butanol (20 mL) was heated to reflux for 24 h under an N_2 atmosphere. On cooling, the volatiles were evaporated under reduced pressure, and the crude product was purified on silica with hexane and ethyl acetate (2:3) as the eluent and two separate compound containing fractions were collected. After removal of the solvent compounds **5b** and **5c** were obtained as colourless crystalline solids. (yield 0.24 g, 18%) and (yield 0.24 g, 22%). ^{1}H NMR (500 MHz, $CDCl_3$): δ = 1.33 (s, 12 H, C*H*$_3$), 7.20-7.23 (m, 3 H), 7.36-7.45 (m, 5 H), 7.71-7.72 (m, 2 H, Ph*H*), 7.76 (t, $^3J_{HH}$ = 7.77 Hz, 1 H, Py*H*), 8.10 (d, $^3J_{HH}$ = 7.85 Hz,

1 H, Py*H*), 8.34 (d, $^3J_{HH}$ = 4.23 Hz, 1 H, Py*H*) ppm. ^{13}C NMR (500 MHz, $CDCl_3$): δ = 25.1 (4-*C*H$_3$), 84.2 (2 C, *C*q),124.1 (Py*C*), 124.6 (Py*C*), 128.2 (Ph*C*), 129.2 (Ph*C*), 129.4 (Ph*C*), 129.5 (Ph*C*), 134.8 (Ph*C*), 136.1 (Ph*C*),), 136.8 (Ph*C*), 147.3 (Py*C*), 149.2 (Py*C*), 154.1 (Tz*C*), 155.7 (Tz*C*) ppm. HRMS (CH_3CN) calcd. for $[C_{50}H_{50}B_2N_8NaO_4]^+$ = 871.4039, found 871.4054.

5c. ^{1}H NMR (500 MHz, $CDCl_3$): δ = 1.37 (s., 12 H, C*H*$_3$), 7.48 (t, $^3J_{HH}$ = 5.95 Hz, 1 H, Py*H*), 7.91 (t, $^3J_{HH}$ = 7.66 Hz, 1 H, Py*H*), 7.96-7.97 (m, 2 H, Ph*H*), 8.21-8.23 (m, 2 H, Ph*H*), 8.33 (d, $^3J_{HH}$ = 7.85 Hz, 1 H, Py*H*), 8.83 (d, $^3J_{HH}$ = 4.72 Hz, 1 H, Py*H*) ppm. ^{13}C NMR (500 MHz, $CDCl_3$): δ = 24.9 (4-*C*H$_3$), 84.3 (2 C, *C*q), 123.3 (Py*C*), 125.7 (Py*C*), 125.8 (Ph*C*), 126.4 (Ph*C*), 135.3 (Ph*C*), 137.2 (Py*C*), 143.6 (Py*C*), 150.4 (Py*C*), 164.0 (Tz*C*), 165.6 (Tz*C*) ppm. HRMS (CH_3CN) calcd. for $[C_{38}H_{40}B_2N_6NaO_6]^+$ = 721.3093, found 721.3120.

5d. This compound was prepared as described for **5a** from **4c** (0.94 g, 2.55 mmol) and **2b** (0.42 g, 3.06 mmol). After removal of the volatiles under reduced pressure the orange liquid was suspended in isopropanol and a precipitate formed which was collected and washed with diethyl ether. Compound **5d** was obtained as a colourless solid. (yield 0.50 g, 46%). ^{1}H NMR (500 MHz, $CDCl_3$): δ = 1.36 (s., 12 H, C*H*$_3$), 7.19-7.23 (m, 3 H), 7.27-7.30 (m, 2 H, Ph*H*), 7.35 (t, $^3J_{HH}$ = 7.44 Hz, 1 H, Py*H*), 7.42-7.44 (m, 2 H, Ph*H*), 7.75 (t, $^3J_{HH}$ = 7.80 Hz, 1 H, Py*H*), 7.79-7.80 (m, 2 H, Ph*H*), 8.08 (d, $^3J_{HH}$ = 7.91 Hz, 1 H, Py*H*), 8.34 (d, $^3J_{HH}$ = 4.83 Hz, 1 H, Py*H*) ppm. ^{13}C NMR (500 MHz, $CDCl_3$): δ = 25.1 (4-*C*H$_3$), 84.5 (2 C, *C*q),124.0 (Py*C*), 124.5 (Py*C*), 127.0 (Ph*C*), 127.5 (Ph*C*), 128.6 (Ph*C*), 129.1 (Ph*C*), 129.9 (Ph*C*), 135.7 (Ph*C*), 136.8 (Ph*C*), 138.5 (Py*C*), 147.2 (Py*C*), 149.2 (Py*C*), 153.9 (Tz*C*), 155.7 (Tz*C*) ppm.

6a. To a solution of **5a** (0.20 g, 0.55 mmol) in methanol (3 mL) was added aqueous KHF_2 (0.70 mL, 4.5 M, 3.12 mmol) and the resulting white slurry was stirred at RT for 30 minutes. The volatiles were then removed under reduced pressure yielding a solid that was recrystallised from acetonitrile, yielding **6a** as a white crystalline solid. (yield 0.14 g, 74%). ^{1}H NMR (500 MHz, DMSO): δ = 3.97 (s, 3 H, C*H*$_3$), 7.47-7.54 (m, 5 H), 8.00 (t, $^3J_{HH}$ = 7.61 Hz, 1 H, Py*H*), 8.17 (d, $^3J_{HH}$ = 7.89 Hz, 1 H, Py*H*), 8.74 (d, $^3J_{HH}$ = 4.23 Hz, 1 H, Py*H*) ppm. ^{13}C NMR (400 MHz, DMSO): δ = 33.8 (*C*H$_3$), 123.4 (Py*C*), 123.6 (Ph*C*), 124.2 (Ph*C*), 127.0 (Ph*C*), 131.6 (Py*C*), 137.5 (Py*C*), 147.9 (Py*C*), 149.1 (Py*C*), 152.5 (Tz*C*), 157.1 (Tz*C*) ppm.

6b. A suspension of **5b** (0.17 g, 0.4 mmol) in methanol (5 mL) was heated at reflux for 30 minutes, yielding a yellow solution. A hot aqueous solution of KHF_2 (0.49 mL, 4.5 M, 2.20 mmol) was added and the resulting mixture was stirred for 30 minutes at reflux during which time a precipitate formed. The precipitated solid was collected and washed with diethyl ether yielding **6b** as a white solid. (yield 0.13 g, 80%). ^{1}H-NMR (400 MHz, DMSO): δ = 7.10-7.11 (m, 2 H, Ph*H*), 7.24 (d, $^3J_{HH}$ = 7.80 Hz, 1

H, Py*H*), 7.28-7.29 (m, 2 H, Ph*H*),7.36-7.41 (m, 5*H*), 7.90 (t, $^3J_{HH}$ = 7.96 Hz, 1 H, Py*H*), 7.97 (d, $^3J_{HH}$ = 7.90 Hz, 1 H, Py*H*), 8.34 (d, $^3J_{HH}$ = 4.23 Hz, 1 H, Py*H)* ppm. ^{13}C NMR (400 MHz, DMSO): δ =123.2 (Py*C*), 124.6 (Ph*C*), 126.8 (Ph*C*), 127.1 (Ph*C*), 128.6 (Ph*C*), 129.5 (Ph*C*), 131.6 (Ph*C*), 131.6 (Ph*C*), 132.2 (Py*C*), 137.0 (Py*C*), 147.0 (Py*C*), 149.3 (Py*C*), 154.0 (Tz*C*), 154.7 (Tz*C*) ppm.

6c. This compound was prepared as described for **6a** from **5c** (0.1 g, 0.30 mmol) and aqueous KHF_2 (0.362 mL, 4.5 M, 1.63 mmol) and after recrystallization from acetonitrile gave **6c** as a white crystalline solid. (yield 0.076 g, 77%). ^{1}H NMR (500 MHz, DMSO): δ = 7.56-7.57 (m, 2 H, Ph*H*), 7.64 (t, $^3J_{HH}$ = 6.21 Hz, 1 H, Py*H*), 7.86-7.87 (m, 2 H, Ph*H*), 8.07 (t, $^3J_{HH}$ = 7.76 Hz, 1 H, Py*H*), 8.25 (d, $^3J_{HH}$ = 7.88 Hz, 1 H, Py*H*), 8.81 (d, $^3J_{HH}$ = 4.79 Hz, 1 H, Py*H*) ppm. ^{13}C NMR (400 MHz, DMSO): δ = 119.9 (Ph*C*), 122.9 (Py*C*), 124.8 (Ph*C*), 126.2 (Py*C*), 132.2 (Ph*C*), 137.8 (Py*C*), 143.0 (Py*C*), 150.3 (Py*C*), 163.1 (Tz*C*), 165.7 (Tz*C*) ppm.

6d. This compound was prepared as described for **6b** from **5d** (0.42 g, 0.99 mmol) and aqueous KHF_2 (1.25 mL, 4.5 M, 5.63 mmol) and was obtained **6d** as a white crystalline solid. (yield 0.38 g, 95%). ^{1}H-NMR (400 MHz, DMSO): δ = 6.99-7.01 (m, 2 H, Ph*H*), 7.29-7.31 (m, 2 H, Ph*H*), 7.33-7.40 (m, 5 H), 7.83 (d,$^3J_{HH}$ = 7.81 Hz, 1 H, Ph*H*), 7.88 (t, $^3J_{HH}$ = 7.78 Hz, 1 H, Py*H*), 8.45 (d, $^3J_{HH}$ = 4.40 Hz, 1 H, Py*H*) ppm. ^{13}C NMR (400 MHz, DMSO): δ =124.2 (Py*C*), 124.4 (Ph*C*), 125.6 (Ph*C*), 127.2 (Ph*C*), 128.4 (Ph*C*), 129.5 (Ph*C*), 131.9 (Ph*C*), 131.9 (Ph*C*), 132.1 (Py*C*), 136.9 (Py*C*), 146.9 (Py*C*), 149.2 (Py*C*), 153.9 (Tz*C*), 154.7 (Tz*C*) ppm.

7a. A mixture of **6a** (0.12 g, 0.35 mmol) and LiOH (0.12 g, 0.35 mmol) in water (3 mL) and acetonitrile (4 mL) was stirred at RT for 24 h and was then acidified to pH 1-2 with saturated NH_4Cl (4 mL) and 1 M hydrochloric acid (2 mL). The white precipitate was collected and recrystalised from hot acetonitrile, yielding **7a** as a white crystalline solid. (yield 0.058 g, 59%). ^{1}H NMR (500 MHz, DMSO): δ = 4.00 (s, 3 H, CH_3), 7.54 (t, $^3J_{HH}$=6.13 Hz,1 H, Py*H*), 7.73-7.75 (m, 2 H, Ph*H*), 7.96-7.98 (m, 2 H, Ph*H*), 8.02 (t, $^3J_{HH}$ =7.86 Hz, 1 H, Py*H*), 8.19 (d, $^3J_{HH}$=7.94 Hz, 1 H, Py*H*), 8.25 (s, 2 H B(O*H*)$_2$), 8.75 (d, $^3J_{HH}$ =4.19 Hz, 1 H, Py*H*) ppm. ^{13}C NMR (500 MHz, DMSO): δ = 34.4 (*C*H$_3$), 124.0 (Py*C*), 124.8 (Py*C*), 128.3 (Ph*C*), 128.8 (Ph*C*), 134.9 (Ph*C*), 135.6 (Ph*C*), 138.0 (Py*C*), 148.1 (Py*C*), 149.6 (Py*C*), 153.3 (Tz*C*), 156.6 (Tz*C*) ppm. HRMS (CH_3OH) calcd. for $[C_{15}H_{16}BN_4O_2]^+$ = 295.1366, found 295.1367; calcd. for $[C_{15}H_{15}BN_4NaO_2]^+$ = 317.1186, found 317.1191.

7b. This compound was prepared as described for **7a** from **6b** (0.11 g, 0.26 mmol) and LiOH (0.038 g, 0.91 mmol). (yield 0.058 g, 65%). ^{1}H-NMR (400 MHz, DMSO): 7.34-7.44 (m, 8 H), 7.71-7.73 (m, 2 H, Ph*H*), 7.92 (t, $^3J_{HH}$= 7.98 Hz, 1 H, Py*H*), 8.01 (d, 7.84 Hz, 1 H, Py*H*), 8.15 (s, 2 H B(O*H*)$_2$), 8.35 (d, 4.40 Hz, 1 H, Py*H*). ^{13}C-NMR: (400 MHz, DMSO): δ = 124.2 (Py*C*), 124.3 (Py*C*), 127.5 (Ph*C*), 128.2 (Ph*C*), 128.2 (Ph*C*), 129.1 (Ph*C*), 129.1 (Ph*C*), 133.9 (Ph*C*), 135.4 (Py*C*), 137.1 (Ph*C*), 146.6

(Py*C*), 149.0 (Py*C*), 153.4 (Tz*C*), 154.9 (Tz*C*) ppm. HRMS (CH_3OH) calcd. for $[C_{20}H_{18}BN_4O_2]^+$ = 357.1523, found 357.1534; calcd. for $[C_{20}H_{17}BN_4NaO_2]^+$ = 379.1342, found 379.1354.

View Article Online
DOI: 10.1039/D0DT02177F

7c. This compound was prepared as described for **7a** from **6c** (0.059 g, 0.18 mmol) and LiOH (0.03 g, 0.63 mmol). (yield 0.025 g, 52%). ^{1}H NMR (500 MHz, DMSO): δ = 7.67 (t, $^3J_{HH}$=6.15 Hz,1 H, Py*H*), 8.01-8.03 (m, 2 H, Ph*H*), 8.07-8.10 (m, 3 H), 8.28 (d, $^3J_{HH}$ =7.83 Hz, 1 H, Py*H*), 8.33 (s, 2 H B(O*H*)$_2$), 8.25 (d, $^3J_{HH}$ =4.70 Hz, 1 H, Py*H*) ppm. ^{13}C NMR (500 MHz, DMSO): δ = 123.6 (Py*C*), 124.9 (Py*C*), 126.1 (Ph*C*), 127.0 (Ph*C*), 135.4 (Ph*C*), 138.4 (Py*C*), 138.4 (Ph*C*), 143.3 (Py*C*), 151.0 (Py*C*), 164.1 (Tz*C*), 165.3 (Tz*C*) ppm. HRMS (CH_3OH) calcd. for $[C_{14}H_{13}BN_3O_3]^+$ = 282.1050, found 282.1047; calcd. for $[C_{14}H_{12}BN_3NaO_3]^+$ = 304.0869, found 304.0874

7d. This compound was prepared as described for **7a** from **6d** (0.1 g, 0.25 mmol) and LiOH (0.036 g, 0.87 mmol). (yield 0.04 g, 47%). ^{1}H-NMR (400 MHz, DMSO): 7.27-7.29 (m, 2 H, Ph*H*),7.33-7.40 (m, 6 H), 7.75-7.77 (m, 2 H, Ph*H*), 7.92 (t,$^3J_{HH}$ =7.73 Hz, 1 H, Py*H*), 7.99 (d, 7.80 Hz, 1 H, Py*H*), 8.30 (s, 2 H B(O*H*)$_2$), 8.35 (d, 4.75 Hz, 1 H, Py*H*). ^{13}C-NMR: (400 MHz, DMSO): δ = 124.2 (Py*C*), 124.3 (Py*C*), 126.9 (Ph*C*), 127.0 (Ph*C*), 128.5 (Ph*C*), 128.6 (Ph*C*), 129.7 (Ph*C*), 134.8 (Ph*C*), 136.8 (Ph*C*), 137.1 (Py*C*), 146.6 (Py*C*), 149.0 (Py*C*), 153.4 (Tz*C*), 154.8 (Tz*C*) ppm. HRMS (CH_3OH) calcd. for $[C_{20}H_{18}BN_4O_2]^+$ = 357.1523, found 357.1466; calcd. for $[C_{20}H_{17}BN_4NaO_2]^+$ = 379.1342, found 379.1276.

8a. To a solution of $[Ir(ppy)_2]_2$ (0.11 g, 0.1 mmol) in dichloromethane (15 mL) and ethanol (5 mL) was added **7a** (56 mg, 0.2 mmol) and the mixture was stirred under an atmosphere of N_2 for 24 h. The volatiles were then removed under reduced pressure and the crude product was purified on silica with dichloromethane and methanol 4:1 as the eluent, yielding complex **8a** was obtained as a yellow crystalline solid. (yield 0.07 g, 43%). ^{1}H-NMR (500 MHz, DMSO): δ= 4.19 (s, 3 H, CH_3), 6.12 (d, $^3J_{HH}$= 7.45 Hz, 1 H), 6.15 (d, $^3J_{HH}$= 7.45 Hz, 1 H), 6.77 (t, $^3J_{HH}$= 7.01 Hz, 1 H), 6.89 (t, $^3J_{HH}$= 7.47 Hz, 1 H), 7.01 (t, $^3J_{HH}$= 7.78 Hz, 1 H), 7.19-7.25 (m, 2 H), 7.58 (d, $^3J_{HH}$= 5.47 Hz, 1 H), 7.63-7.65(m, 2 H), 7.72 (t, $^3J_{HH}$= 5.72 Hz, 1 H), 7.80 (d, $^3J_{HH}$= 7.60 Hz, 1 H), 7.88-7.98 (m, 7 H), 8.23 (t, $^3J_{HH}$= 7.56 Hz, 2 H), 8.29 (t, $^3J_{HH}$= 7.40 Hz, 2 H), 8.40 (s, 2 H, B(O*H*)$_2$), 8.61 (d, $^3J_{HH}$= 8.19 Hz, 1 H) ppm. ^{13}C-NMR (500 MHz, DMSO): δ = 79.7, 119.5, 119.7, 120.0, 120.2, 122.0, 122.8, 124.0, 124.3, 124.8, 124.9, 125.0, 125.4, 125.5, 125.6, 126.3, 129.0, 130.5, 131.5, 135.0, 138.8, 139.0, 140.4, 144.2, 144.7, 145.6, 148.0, 149.6, 150.6, 151.4, 156.9, 158.5, 167.3, 167.7 ppm. HRMS (CH_3CN) calcd. for $[C_{36}H_{29}BIrN_6O_2]^+$ = 781.2074, found 781.2083.

8b. This compound was prepared as described for **8a** from $[Ir(ppy)_2]_2$ (0.072 g, 0.067 mmol) and **7b** (0.046 g, 0.134 mmol). The crude product was purified by the diffusion of vapours between an acetonitrile solution of the crude product and diethyl ether, yielding complex **8b** as a yellow

crystalline solid. (yield 0.03 g, 25%). ^{1}H-NMR (500 MHz, DMSO): δ= 6.13 (d, $^{3}J_{HH}$ = 7.56, 1 H), 6.19 (d, $^{3}J_{HH}$ = 7.59 Hz, 1 H), 6.80 – 6.83 (m, 2 H), 6.88-6.95 (m, 2 H), 7.01 (t, $^{3}J_{HH}$ = 7.48 Hz, 1 H), 7.25 (t, $^{3}J_{HH}$ = 6.60 Hz, 1 H), 7.30 – 7.34 (m, 3 H), 7.62 (t, $^{3}J_{HH}$ = 6.15 Hz, 1 H), 7.69-7.79 (m, 6 H), 7.84-7.92 (m, 5 H), 7.96-8.02 (m, 3 H), 8.11 (d,$^{3}J_{HH}$ = 5.80, 2 H), 8.24-8.26 (m, 1 H), 8.25 (s, 2 H B(O*H*)$_2$) ppm. ^{13}C-NMR: (400 MHz, DMSO): δ =119.7, 119.8, 121.7, 122.4, 123.1, 123.8, 124.1, 124.5, 124.6, 125.0, 127.3, 128.7, 128.9, 129.0, 129.4, 130.2, 131.0, 131.0, 131.2, 134.2, 136.3, 138.5, 138.7, 139.8, 143.9, 144.3, 144.4, 147.2, 149.6, 150.3, 150.4, 151.1, 155.7, 156.8, 166.7, 167.2 ppm. HRMS (CH_3CN) calcd. for $[C_{41}H_{31}BIrN_6O_2]^+$ = 843.2231, found 843.2249.

8c. This compound was prepared as described for **8a** from $[Ir(ppy)_2]_2$ (0.10 g, 0.095 mmol) and **7c** (0.051 g, 0.19 mmol). The dark orange crude product was recrystallized from acetonitrile, yielding complex **8c** as an orange crystalline solid. (yield 0.13 g, 85%). ^{1}H-NMR (500 MHz, DMSO): δ= 6.12 (t, $^{3}J_{HH}$ = 9.60, 2 H), 6.83 (t, $^{3}J_{HH}$ = 7.42 Hz, 1 H), 6.91 (t, $^{3}J_{HH}$ = 7.42 Hz, 1 H), 6.96 (t, $^{3}J_{HH}$ = 7.42 Hz, 1 H), 7.02 (t, $^{3}J_{HH}$ = 7.58 Hz, 1 H), 7.17 – 7.21 (m, 2 H), 7.65 (d, $^{3}J_{HH}$ = 5.30, 1 H), 7.82-7.86 (m, 3 H), 7.89 (d, $^{3}J_{HH}$ = 7.60 Hz, 1 H), 7.95 (t, $^{3}J_{HH}$ = 7.90 Hz, 2 H), 8.01 (d,$^{3}J_{HH}$ = 8.16, 2 H), 8.10 (d,$^{3}J_{HH}$ = 8.24, 2 H), 8.24 (d,$^{3}J_{HH}$ = 8.20, 2 H), 8.27 (d,$^{3}J_{HH}$ = 5.66, 1 H), 8.38-8.41 (m, 1 H), 8.39 (s, 2H B(O*H*)$_2$), 8.70 (d,$^{3}J_{HH}$ = 7.91, 1 H) ppm. ^{13}C-NMR: (400 MHz, DMSO): δ = 119.6, 119.8, 122.1, 122.7, 123.2, 123.7, 123.9, 124.6, 125.0, 125.9, 126.2, 129.5, 130.2, 130.8, 131.3, 135.0, 138.7, 138.9, 140.5, 141.1, 144.1, 144.2, 144.8, 147.3, 150.2, 150.8, 151.3, 166.2, 166.8, 166.9, 168.4 ppm. HRMS (CH_3CN) calcd. for $[C_{35}H_{26}BIrN_5O_3]^+$ = 768.1758, found 768.1771.

8d. This compound was prepared as described for **8a** from $[Ir(ppy)_2]_2$ (0.084 g, 0.079 mmol) and **7d** (0.054 g, 0.16 mmol). The yellow crude product was recrystallized from acetonitrile, yielding complex **8d** as a yellow crystalline solid. (yield 0.11 g, 79%). ^{1}H-NMR (500 MHz, DMSO): ^{1}H-NMR (500 MHz, DMSO): δ= 6.14 (d, $^{3}J_{HH}$ = 3.62, 1 H), 6.19 (d, $^{3}J_{HH}$ = 3.62 Hz, 1 H), 6.79 – 6.85 (m, 2 H), 6.88-6.94 (m, 2 H), 7.01 (t, $^{3}J_{HH}$ = 7.43 Hz, 1 H), 7.25 (t, $^{3}J_{HH}$ = 6.54 Hz, 1 H), 7.30 – 7.39 (m, 5 H), 7.44 (t, $^{3}J_{HH}$ = 7.06 Hz, 1 H), 7.62 (t, $^{3}J_{HH}$ = 6.45 Hz, 1 H), 7.72 (d, $^{3}J_{HH}$ = 5.76, 1 H), 7.81 – 7.90 (m, 5 H), 7.96 – 8.01 (m, 3 H), 8.09 – 8.13 (m, 3 H), 8.25 (d,$^{3}J_{HH}$ = 4.23, 2 H), 8.46 (s, 2 H B(O*H*)$_2$) ppm. ^{13}C-NMR: (400 MHz, DMSO): δ = 119.7, 119.8, 121.7, 122.4, 123.0, 123.8, 124.0, 124.5, 124.6, 125.0, 127.3, 128.7, 128.9, 129.0, 129.4, 130.2, 131.0, 131.0, 131.2, 134.2, 136.3, 138.5, 138.7, 139.8, 143.9, 144.3, 144.4, 147.2, 149.6, 150.3, 150.4, 151.1, 155.7, 156.8, 166.7, 167.2 ppm. HRMS (CH_3CN) calcd. for $[C_{41}H_{31}BIrN_6O_2]^+$ = 843.2231, found 843.2245.

Conflict of Interests

There are no conflicts of interest to declare.

Acknowledgements

We acknowledge generous allocating of computing resources by NCI, Intersect, and La Trobe University.

View Article Online
DOI: 10.1039/D0DT02177F

Electronic Supplementary Information (ESI)

Synthetic description for compounds **1a**, **1b**, **2a**, **2b**, **3a** and **3b**, further X-ray diffraction details, mass spectra for compounds **5b**, **5c**, **7a**, **7b**, **7c**, **7d**, **8a**, **8b**, **8c** and **8d** and luminescence titration results for compounds **8a**, **8b** and **8c**.

References

1. X. Sun and T. D. James, *Chem. Rev.*, 2015, **115**, 8001-8037.
2. H. E. Murrey and L. C. Hsieh-Wilson, *Chem. Rev.*, 2008, **108**, 1708-1731.
3. P. Luppi, V. Cifarelli and J. Wahren, *Pediatr. Diabetes.*, 2011, **12**, 276-292.
4. T. E. R. F. Collaboration, *The Lancet*, 2010, **375**, 2215-2222.
5. X. Sun, W. Zhai, J. S. Fossey and T. D. James, *Chem. Comm.*, 2016, **52**, 3456-3469.
6. H.-C. Wang and A.-R. Lee, *J. Food. Drug. Anal.*, 2015, **23**, 191-200.
7. A. Stephenson-Brown, A. L. Acton, J. A. Preece, J. S. Fossey and P. M. Mendes, *Chem. Sci.*, 2015, **6**, 5114-5119.
8. X. Sun, B. Zhu, D.-K. Ji, Q. Chen, X.-P. He, G.-R. Chen and T. D. James, *ACS Appl. Mater.*, 2014, **6**, 10078-10082.
9. G. Fang, H. Wang, Z. Bian, J. Sun, A. Liu, H. Fang, B. Liu, Q. Yao and Z. Wu, *RSC. Adv.*, 2018, **8**, 29400-29427.
10. O. S. Wolfbeis, I. Klimant, T. Werner, C. Huber, U. Kosch, C. Krause, G. Neurauter and A. Dürkop, *Sens. Actuators B Chem.*, 1998, **51**, 17-24.
11. D. R. Cary, N. P. Zaitseva, K. Gray, K. E. O'Day, C. B. Darrow, S. M. Lane, T. A. Peyser, J. H. Satcher, W. P. Van Antwerp, A. J. Nelson and J. G. Reynolds, *Inorg. Chem.*, 2002, **41**, 1662-1669.
12. H. S. Mader and O. S. Wolfbeis, *Microchim. Acta.*, 2008, **162**, 1-34.
13. Z. Murtaza, L. Tolosa, P. Harms and J. R. Lakowicz, *J.Fluoresc.*, 2002, **12**, 187-192.
14. M. J. Deetz and B. D. Smith, *Tetrahedron Lett.*, 1998, **39**, 6841-6844.
15. V. Wing-Wah Yam and A. Sze-Fai Kai, *Chem. Com.*, 1998, 109-110.
16. T. Mizuno, T. Fukumatsu, M. Takeuchi and S. Shinkai, *J. Chem. Soc., Perkin Trans. 1*, 2000, 407-413.
17. G. J. Barbante, E. H. Doeven, P. S. Francis, B. D. Stringer, C. F. Hogan, P. R. Kheradmand, D. J. D. Wilson and P. J. Barnard, *Dalton Trans.*, 2015, **44**, 8564-8576.
18. G. J. Barbante, P. S. Francis, C. F. Hogan, P. R. Kheradmand, D. J. D. Wilson and P. J. Barnard, *Inorg. Chem.*, 2013, **52**, 7448-7459.
19. L. M. Quan, B. D. Stringer, M. A. Haghighatbin, J. Agugiaro, G. J. Barbante, D. J. Wilson, C. F. Hogan and P. J. Barnard, *Dalton. Trans.*, 2019, **48**, 653-663.
20. B. D. Stringer, L. M. Quan, P. J. Barnard, D. J. D. Wilson and C. F. Hogan, *Organometallics.*, 2014, **33**, 4860-4872.
21. B. D. Stringer, L. M. Quan, P. J. Barnard and C. F. Hogan, *ChemPhotoChem.*, 2018, **2**, 27-33.
22. R. E. Karmis, S. Carrara, A. A. Baxter, C. F. Hogan, M. D. Hulett and P. J. Barnard, *Dalton. Trans.*, 2019, **48**, 9998-10010.
23. L. M. Quan, A. I. Mechler and P. J. Barnard, *J. Inorg. Biochem.*, 2020, **206**, 111047.
24. M. H. Klingele and S. Brooker, *Eur. J. Org. Chem.*, 2004, **2004**, 3422-3434.
25. H. D. Porter, *J. Am. Chem. Soc.*, 1954, **76**, 127-128.
26. T. S. Jagodziński, *Chem. Rev.*, 2003, **103**, 197-228.

27. A. K. Yuen and C. A. Hutton, *Tetrahedron. Lett.*, 2005, **46**, 7899-7903.
28. K. Durka, K. N. Jarzembska, R. Kamiński, S. Luliński, J. Serwatowski, K. Woźniak and design, *Cryst. Growth Des.*, 2013, **13**, 4181-4185.
29. C. S. Mak, A. Hayer, S. I. Pascu, S. E. Watkins, A. B. Holmes, A. Köhler and R. H. Friend, *Chem. Commun.*, 2005, 4708-4710.
30. J. Zhang, L. Zhou, H. A. Al-Attar, K. Shao, L. Wang, D. Zhu, Z. Su, M. R. Bryce and A. P. Monkman, *Adv. Funct. Mater.*, 2013, **23**, 4667-4677.
31. T. U. Connell, J. M. White, T. A. Smith and P. S. Donnelly, *Inorg. Chem.*, 2016, **55**, 2776-2790.
32. M. Felici, P. Contreras-Carballada, Y. Vida, J. M. Smits, R. J. Nolte, L. De Cola, R. M. Williams and M. C. Feiters, *Chem-Eur. J.*, 2009, **15**, 13124-13134.
33. J. Yoon and A. W. Czarnik, *J. Am. Chem. Soc.* , 1992, **114**, 5874-5875.
34. R. Nishiyabu, Y. Kubo, T. D. James and J. S. Fossey, *Chem. Commun.*, 2011, **47**, 1106-1123.
35. J. H. Hartley, M. D. Phillips and T. D. James, *New J. Chem.*, 2002, **26**, 1228-1237.
36. X. Wu, Z. Li, X.-X. Chen, J. S. Fossey, T. D. James and Y.-B. Jiang, *Chem. Soc. Rev.*, 2013, **42**, 8032-8048.
37. N. Ni, S. Laughlin, Y. Wang, Y. Feng, Y. Zheng and B. Wang, *Bioorgan. Med. Chem.*, 2012, **20**, 2957-2961.
38. Y.-J. Huang, W.-J. Ouyang, X. Wu, Z. Li, J. S. Fossey, T. D. James and Y.-B. Jiang, *J. Am. Chem. Soc.*, 2013, **135**, 1700-1703.
39. J. P. Lorand and J. O. Edwards, *J. Org. Chem.*, 1959, **24**, 769-774.
40. S. J. Angyal, in *Advances in Carbohydrate Chemistry and Biochemistry*, eds. R. S. Tipson and D. Horton, Academic Press, 1984, vol. 42, pp. 15-68.
41. S. J. Angyal, in *Advances in Carbohydrate Chemistry and Biochemistry*, ed. D. Horton, Academic Press, 1991, vol. 49, pp. 19-35.
42. W. Yang, H. He and D. G. Drueckhammer, *Angew. Chem., Int. Ed.*, 2001, **40**, 1714-1718.
43. X.-D. Xu, H. Cheng, W.-H. Chen, S.-X. Cheng, R.-X. Zhuo and X.-Z. Zhang, *Sci. Rep.*, 2013, **3**, 2679.
44. CrysAlisPro, 2011.
45. G. M. Sheldrick, *Acta Crystallogr., Sect. A: Found. Crystallogr.*, 2008, **64**, 112-122.
46. O. V. Dolomanov, L. J. Bourhis, R. J. Gildea, J. A. K. Howard and H. Puschmann, *J. Appl. Crystallogr.*, 2009, **42**, 339-341.
47. M. J. Frisch, G. W. Trucks, H. B. Schlegel, G. E. Scuseria, M. A. Robb, J. R. Cheeseman, G. Scalmani, V. Barone, G. A. Petersson, H. Nakatsuji, X. Li, M. Caricato, A. V. Marenich, J. Bloino, B. G. Janesko, R. Gomperts, B. Mennucci, H. P. Hratchian, J. V. Ortiz, A. F. Izmaylov, J. L. Sonnenberg, D. Williams-Young, F. Ding, F. Lipparini, F. Egidi, J. Goings, B. Peng, A. Petrone, T. Henderson, D. Ranasinghe, V. G. Zakrzewski, J. Gao, N. Rega, G. Zheng, W. Liang, M. Hada, M. Ehara, K. Toyota, R. Fukuda, J. Hasegawa, M. Ishida, T. Nakajima, Y. Honda, O. Kitao, H. Nakai, T. Vreven, K. Throssell, J. A. Montgomery, J. E. Peralta, F. Ogliaro, M. J. Bearpark, J. J. Heyd, E. N. Brothers, K. N. Kudin, V. N. Staroverov, T. A. Keith, R. Kobayashi, J. Normand, K. Raghavachari, A. P. Rendell, J. C. Burant, S. S. Iyengar, J. Tomasi, M. Cossi, J. M. Millam, M. Klene, C. Adamo, R. Cammi, J. W. Ochterski, R. L. Martin, K. Morokuma, Ö. Farkas, J. B. Foresman and D. J. Fox,Gaussian 16, Revision B. 01, 2016.
48. C. Adamo and V. Barone, *J. Chem. Phys.*, 1998, **108**, 664-675.
49. A. Schafer, H. Horn and R. Ahlrichs, *J. Chem. Phys.*, 1992, **97**, 2571-2577.
50. A. Schafer, C. Huber and R. Ahlrichs, *J. Chem. Phys.*, 1994, **100**, 5829-5835.
51. A. D. Becke, *Phys. Rev. A: Gen. Phys.*, 1988, **38**, 3098-3100.
52. J. P. Perdew, *Phys. Rev. B*, 1986, **33**, 8822-8824.
53. J.-D. Chai and M. Head-Gordon, *Phys. Chem. Chem. Phys.*, 2008, **10**, 6615-6620.
54. J. Tomasi, B. Mennucci and R. Cammi, *Chem. Rev.*, 2005, **105**, 2999-3093.
55. A. V. Marenich, C. J. Cramer and D. G. Truhlar, *J. Phys. Chem. B*, 2009, **113**, 6378-6396.

View Article Online
DOI: 10.1039/D0DT02177F

View Article Online
DOI: 10.1039/D0DT02177F